Experimental investigation of the wake behind a model of wind turbine in a water flume

Okulov, Valery; Naumov, Igor; Kabardin, I.; Mikkelsen, Robert Flemming; Sørensen, Jens Nørkær

Published in:
Journal of Physics: Conference Series (Online)

Link to article, DOI:
10.1088/1742-6596/555/1/012080

Publication date:
2014

Document Version
Publisher's PDF, also known as Version of record

Experimental investigation of the wake behind a model of wind turbine in a water flume

Experimental investigation of the wake behind a model of wind turbine in a water flume

V L Okulov[1], I N Naumov[2], I Kabardin[2], R Mikkelsen[1] and J N Sørensen[1]

[1]Dep. Wind Energy, Technical University of Denmark, 2800 Lyngby, Denmark
[2] Institute of Thermophysics, SB RAS, Lavrentyev Ave. 1,Novosibirsk 630090, Russia

E-mail: vaok@dtu.dk

Abstract. The flow behind the model of wind turbine rotor is investigated experimentally in a water flume using Particle Image Velocimetry. The study carried out involves rotors of three bladed wind turbine designed using Glauert's optimization. The transitional regime, generally characterized as in between the regime governed by stable organized vortical structures and the turbulent wake, develops from disturbances of the tip and root vorticies through vortex paring and further complex behaviour towards the fully turbulent wake. Our PIV measurements pay special attention to the onset of the instabilities. The near wake characteristics (development of expansion, tip vortex position, deficit velocity and rotation in the wake) have been measured for different tip speed ratio to compare with main assumptions and conclusions of various rotor theories.

1. Introduction

The development of studies on rotor aerodynamics (screw, propeller, wind turbine etc.) was usually closely related to an intensive growth in related industry: steamship navigation, aviation and wind energy now. The level of theoretical research (theories of actuator disk by Rankin and Froude [1]; vortex theory by Joukowsky [2] and Betz [3]; Goldstein's solution [4]; novel analytical solutions by Okulov and Sørensen [5]; etc.) was always ahead of developed experimental investigations of the flows. Sometimes this constituted a barrier for confirming theories of rotors. In some cases, incorrect interpretations of observations fueled the development of incorrect concepts. For example, the incorrect perception and interpretation of Parson's experiments delayed by more than 30 years the Froude's theory of actuator disk [6]. Indeed, the flow behind a rotor is complex and unsteady which requires special tools and techniques for measurements.

The first experiments in this field used the simplest experimental methods: air-bubble visualization of the vortex structures behind ship propellers in water [7] or observing flow patterns by inclinations of paper strips or fibers in flow around rotor [8]. These Flamm's and Ryabushinsky's visualizations have been used in Joukovsky's analysis resulting in his vortex theory [2]. A long time after than researchers were studied the average characteristics of swirl flow in the rotor wake [9]. The understanding of the averaged flow inspired the development of several semi-empirical and engineering methods for calculation of rotors. But this approach has limitations and could not live up to the expectations of being a driver of theory development or verification of simulations because the process of averaging inevitably led to the loss of important information about the space form of the vortical structures downstream the rotor. The information was available from the flow visualization in the early stage and it was thus used for construction of the classic vortex theory of rotors.

The first detailed data were provided by intrusive methods with fast response pressure sensor and hot wires [10, 11]. Later non-intrusive tools were invented and applied, e.g. stroboscopic visualization, the laser Doppler anemometer and Particle Image Velocimetry [9]. The last method became the background to start the European project "MEXICO" [12]. In these investigations, the researches pursued a large-scale study of rotor flow in a wind tunnel. Although the data processing of the flow investigations is still in progress, the first comparison of experimental data to computer simulations do not show good agreement with theory [13]. A more complete study of the corresponding flow structures downstream a ship propeller and hydro-turbine was based on velocity visualizations in combination with LDA measurements for velocity field with phase averaging [14, 15]. This progress in optical-based measurement techniques assured desired accuracy of measuring velocity but there was not enough data to provide a better understanding of the underlying physics of wind turbine aerodynamics.

The objective of the current work is PIV investigation and recording of the 3D velocity field in transverse cross section in a water channel downstream a three-blade rotor of a windmill model. The near wake characteristics (development of expansion, tip vortex position, deficit velocity and rotation in the wake) will be measured for different tip speed ratio to compare with main assumptions and conclusions of various rotor theories.

2. Experimental Method

A model of three-blade rotor was specially manufactured for qualitative and quantitative flow visualizations downstream of the rotor (Fig. 1). The rotor diameter was $2R = 0.376$ m, and the blades length was 0.159 m with the CD7003 blade profile adopted from [16]. The blade chord and angle of attack along span were calculated by the Glauert's theory for an optimal windmill [17] with the tip speed ratio $\lambda = 5$, where $\lambda = \Omega R/V$, and Ω is angular speed of the rotor. The angle of attack of the blade was fixed in each tested cases. The Reynolds number was calculated as $Re = \rho\Omega Rb/\mu$. Here ρ and μ are the density and dynamic viscosity of the working fluid (tap water), b is the length of the blade chord (1 cm). The Reynolds number for all experiments was about 20 000 at the working temperature of 20º C in the water flume. The water flume had a length of 35 m, a width of 3 m and the operative height was 0.9 m. A 3-m long test section with transparent walls of optical resolution was installed at a distance of 20 m from the channel inlet; the test section walls and bottom were made of glass. At first the water flow in flume moves through a confusor and a honeycomb (a cell-shaped geometry for linearization of flow velocity throughout the channel cross section). After this flow regularization the horizontal and vertical velocity profiles were measured in cross sections of the flume. The velocity profiles of the flume are shown on Fig. 2, with the velocity profile from the wall (1) and from the bottom (2) in middle position of flume.

Figure 1. A windmill rotor model in an empty water flume

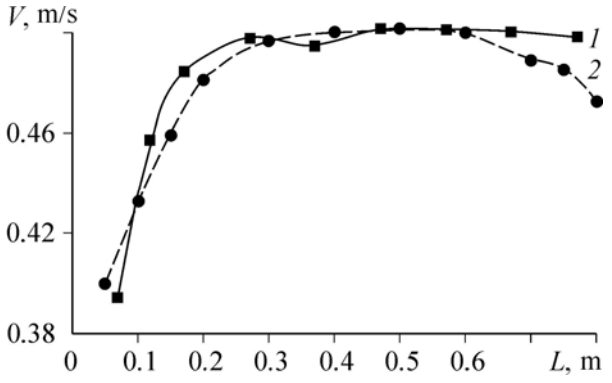

Figure 2. Examples of velocity profile from the wall (1) and the bottom (2) in cross sections of the flume.

This indicates that the velocity profile is constant 0.25 m from the edges and across the flume in the region 0.25-0.65 m above the bottom. The variations of a velocity profile of the incoming water flow were less than 3 % during all experiments. It was tested by an independent velocimeter OTT Z400 on the entrance of the flume. Two regimes with initial speed V = 0.38 and 0.5 m/s were investigated.

The rotor was mounted by 0.6 m long arm which after bend was attached to a platform placed behind them in top of the test section (Fig. 3). The rotor axis was positioned at a height of 0.5 m from the channel bottom and 1.5 m away from the channel walls in accordance with distribution of initial velocity profiles (Fig. 2). The rotor was driven by a JVL Industri Elektronik MAC400 servo motor at a constant r.p.m. The torque of the motor was transferred to the rotor axis via a rigid gear transmission. The software "MacTalk" used to control the motor ensured a proper rotor r.p.m. f within 2 % accuracy. Table 1 indicates the rotor r.p.m. for different tip speed ratios λ for incoming flow velocity V=0.38 m/s.

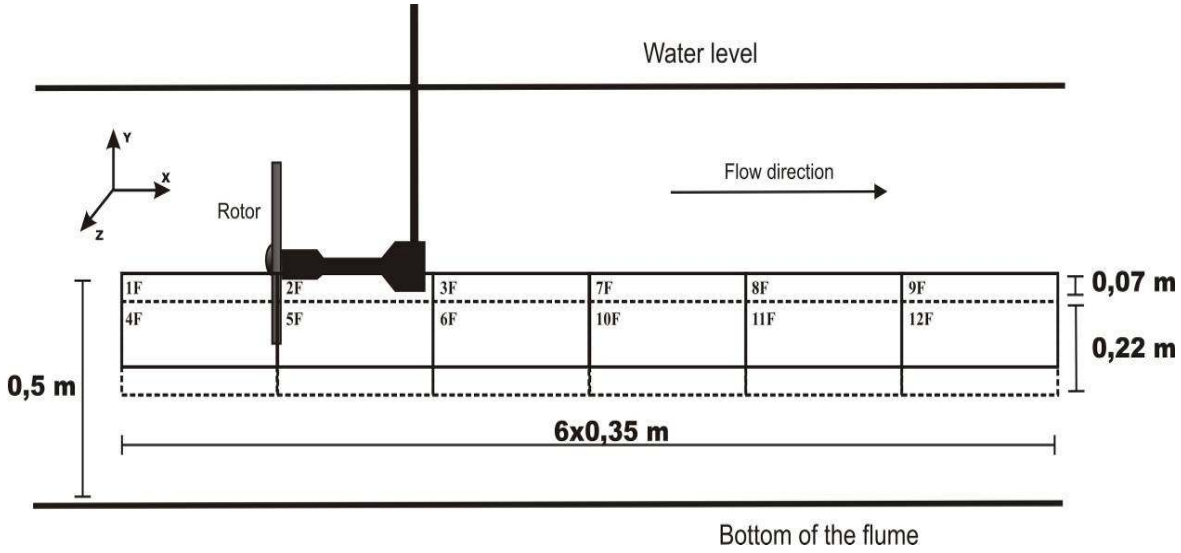

Figure 3. Sketch of setup and the 12 testing windows in the transverse cross section for 3 component PIV measurements of the velocity field

Table 1.

f (r.p.m.)	λ
60	3
80	4
100	5
120	6
140	7
160	8
180	9

The flow downstream rotor has a well-pronounced 3D vortex structure which rotates (Fig. 4). This unsteady flow complicates extremely any kind of measurements. That is, in particular, true regarding diagnostics of instantaneous flow patterns when a large number of measurement points are tested simultaneously. The application of PIV techniques allows us to record rapid and simultaneous multi-point measurements and study instantaneous flow patterns. However, that is possible only within a 2D plane light sheet crossing the tested flow zone [18]. For example, in a cross section passing through a geometric axis of the rotor the light sheet should be oriented perpendicularly to the rotation plane of the rotor. This means the light sheet is normal to circumferential component of velocity vector (which has a high magnitude and uneven distribution). In the time between two pulses, particles may leave or enter the light sheet, which can cause erroneous correlations and produce random errors in the resulting vector fields. One can reduce the variability using better converged statistics by averaging over an increasing amount of realizations. As it was shown in [19] on example of the similar swirling flow generated by rotating top in a cavity, this approach works well in meridian cross-section for stationary regimes. That reduces the statistical errors and shows good agreement with other diagnostic tools and results from computer flow simulation. However in our case, when we deal with time-varying flows, this type of averaging can smooth out the non-stationary features of a flow and accumulate the drifting error. A solution to this problem is to perform phase statistic averaging as was done e.g. in [20]. This assumes that the flow pattern is periodically repeated with each rotor blade passage. Hence, one has to link the phase acquisition to the frequency of the blades passages (e.g. captured at the moment of blade travel through the lowest point). To accomplish this, an angular encoder ROTACAM ASR58 was installed on the rotor shaft. The encoder generated a stroboscopic signal when a blade passed through the light sheet at the moment of time when the instantaneous velocity field was to be measured.

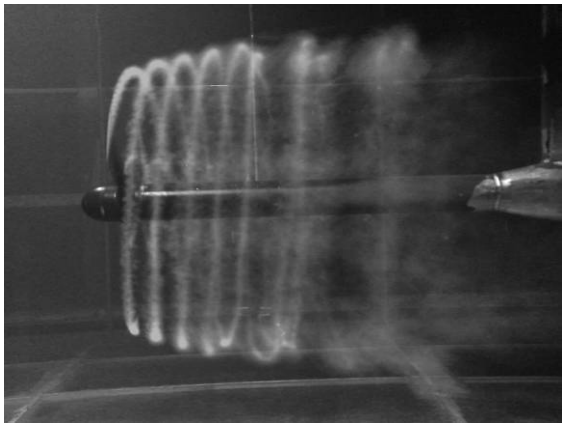

Figure 4. Example of the flow visualization of the 3D vortex structure behind rotor ($\lambda = 8$)

The flow studies by the Dantec Stereoscopic PIV system which gives all three velocity components throughout widow of the light sheet. An Nd:YAG laser was used as a light source with the following characteristics: 120 mJ of energy in a single pulse, the wavelength is 532 nm, operation frequency is 15 Hz. The 2 mm thick light sheet was sent in vertically into the channel from the bottom and directly aiming at the rotor axis (see Fig. 5a). The images were recorded by two Dantec HiSense II cameras with 1344÷1024 pixels resolution. The 3D velocity field was calculated using Dantec Dynamic Studio 2.21. The cameras were placed perpendicularly to each other on the different sides of the flume and at angle of 45º to the walls (Fig. 5b). Water-filled optical prisms were installed between the cameras and the test section to reduce the distortions having from the camera inclination to the wall. Since the cameras were placed at an angle to the light sheet, the focus plane was adjusted using Scheimpflug adapters. The experimental errors has been minimized during calibration and test experiments by finding a trade-off between width of the light sheet, and the time between pulses, and the interrogation

area. The stereoscopic PIV system was calibrated using a target with a well-defined dot-pattern which was translated and registered by the cameras in a number of well-defined positions at the light sheet. The measuring error of stereoscopic PIV was at the level of 3÷5 %.

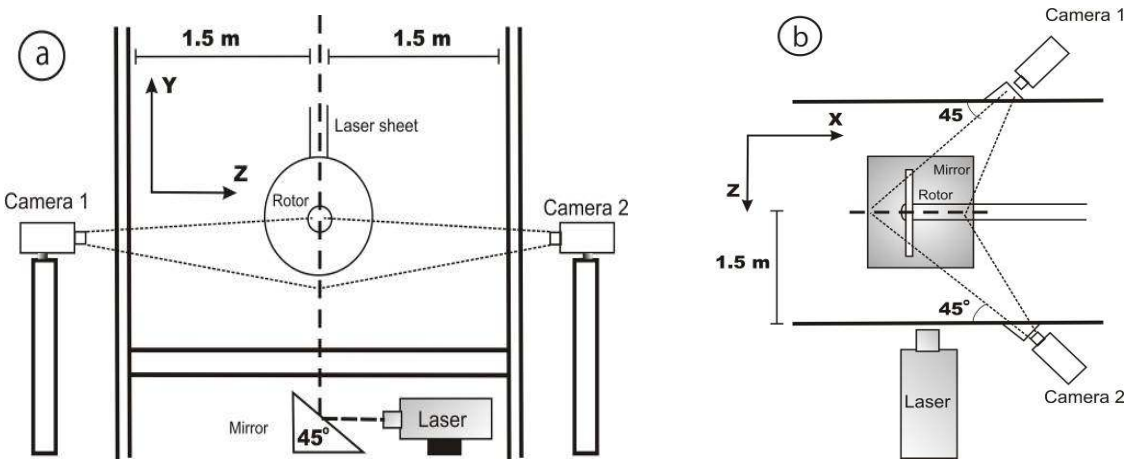

Figure 5. Sketch of stereoscopic PIV measurements in the transverse cross section

We divided the area of investigation into 12 separate windows of 0.22*0.35 m to obtain higher resolution for vortex structures in the rotor wake (see Fig. 3). The choice of the window positions and size were based on previous visualization results (Fig. 4) and adapted to the typical size of the tip vortices with resolution 2.5 mm. The windows were overlapped by 0.01 m to ensure that no gaps occur between the measurement positions. The stereoscopic PIV system was immobile while the model of rotor installed on the movable platform was shifted and then fixed to measure in new measuring window. This movable platform was used to move the rotor in both vertical and horizontal direction to avoid new calibration procedure because the optical system of the SPIV is quite sensitive to any disbalance in disposition of light sheet and cameras. The final size of the total 3D velocity field is 2.06*0.29 m, excluding overlap zones for minimizing boundary errors.

For each measuring window the ultimate velocity field was obtained by phase averaging of 100 realizations, which were recorded in the moment of a triggered signal by a light pulse per the one revolution of the rotor. The angular encoder ROTACAM ASR58 with angular resolution 0.1° installed on the rotor hub has formed the triggered pulse when one of the blades passed through the light sheet. The stochastic errors vanish by this phase averaging. Moreover, this approach eliminates the drifting error due to non-stationary flow regimes too. The processing of the images has been resulted in three velocity components in the tested plane. Then the data for all windows have been merged with uniform cutting of the overlap zones to yield the total velocity field.

3. Development of vortex system behind rotor

The flow structures are well known (Fig. 4) and have been further illustrated for different operating regimes (Fig. 6). This dye visualization well indicates a structure of the tip vortices which are perfectly imagined as continuous curves with a very nearly perfect helical shape with a slight expansion in the axial direction downstream of the rotor. The vortex pitch decreases with grow of the tip speed ratio λ.

These photos prove an onset of initial disturbances for all operating regimes on the early development of the wake. These visualizations can indicate the initial point of the transitional regime. That regime generally characterized as in between the regime governed by stable organized vortical structures in the near or far wakes and the turbulent wake, develops from disturbances of the tip vortices through vortex paring and further complex behavior towards the fully turbulent wake.

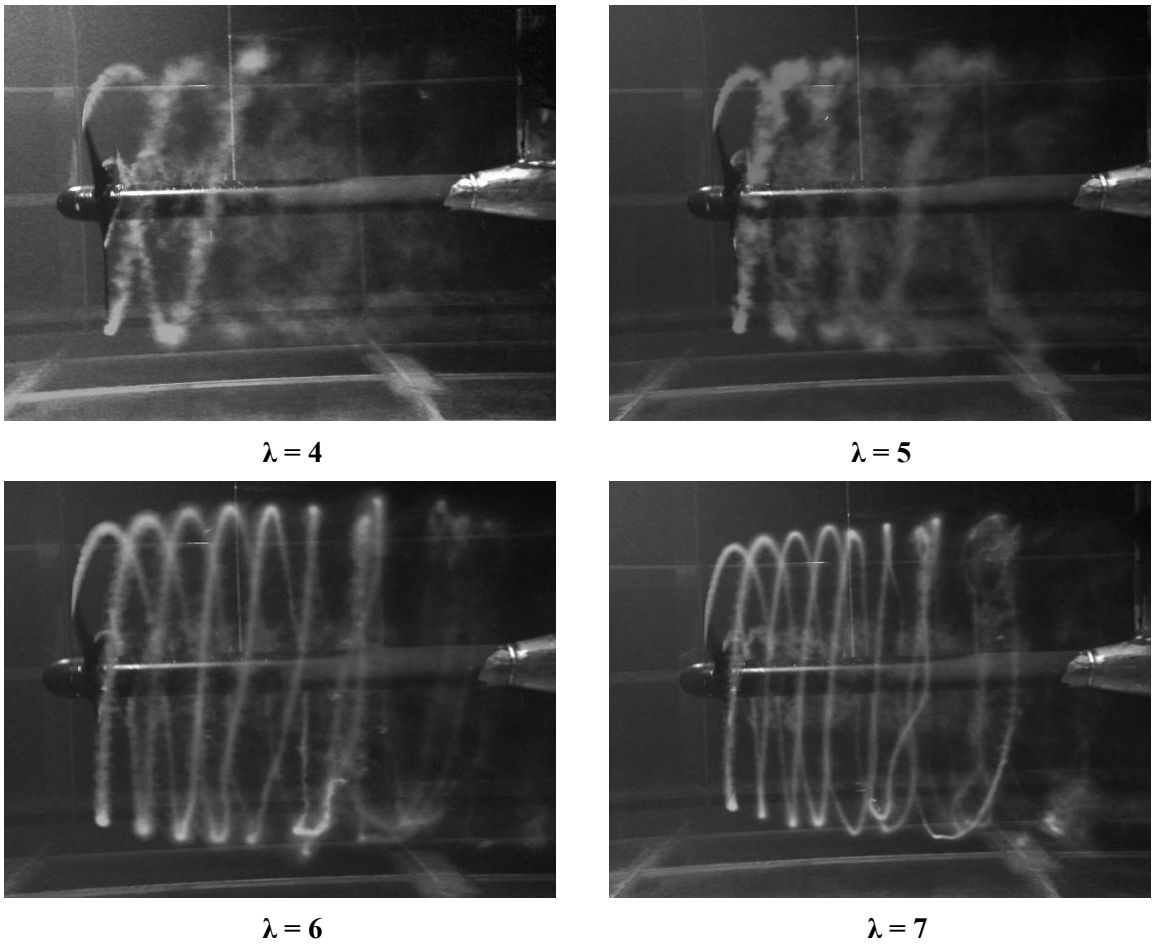

Figure 6. Visualization of the 3-D vortex structure behind rotor

Unfortunately the visualization could not use to detect the subsequent transition to a full turbulent wake stage and even in the stable near/far wake it could not indicate a full vortex structure behind rotor which usually consists from tip, hub (root) vortices around the rotor axis and helical vortex sheet formed at the trailing edge of the blade. However information about the total vortex structure of the wake is very important because the hub vortex, which embraces the rotor spindle, induces an azimuthal rotation flow but the helical system from tip vortex and partially vortex sheet compensates this flow rotation and in additional they induce a strong reversal flow inside the wake. In additional the visual observations could not use to indicate full development of the wake. From the traditional point of view there are four wake stages: near wake with a stable expanding vortex structure in which axial velocity decrease from 2/3 to 1/3 of wind speed; far wake with a stable invariable vortex structure and speed; the transitional regime in the wake with unstable destruction of the vortex structure: and the turbulent wake. For both reasons our PIV measurements pay special attention to study these nonvisual vortex structures and wake stages. Figs. 7 and 8 shows phase averaged and ensemble averaged 3D velocity fields for two operational modes with tip speed ratios $\lambda = 5$ and 6. For both tip speed ratios, iso-contour maps of each phase averaged velocity component (Fig. 7) are plotted at a moment when the rotor blade passes through the laser sheet and the ensemble averaged ones were collected from the all instantaneous velocity field at different blade positions with step of 15º.

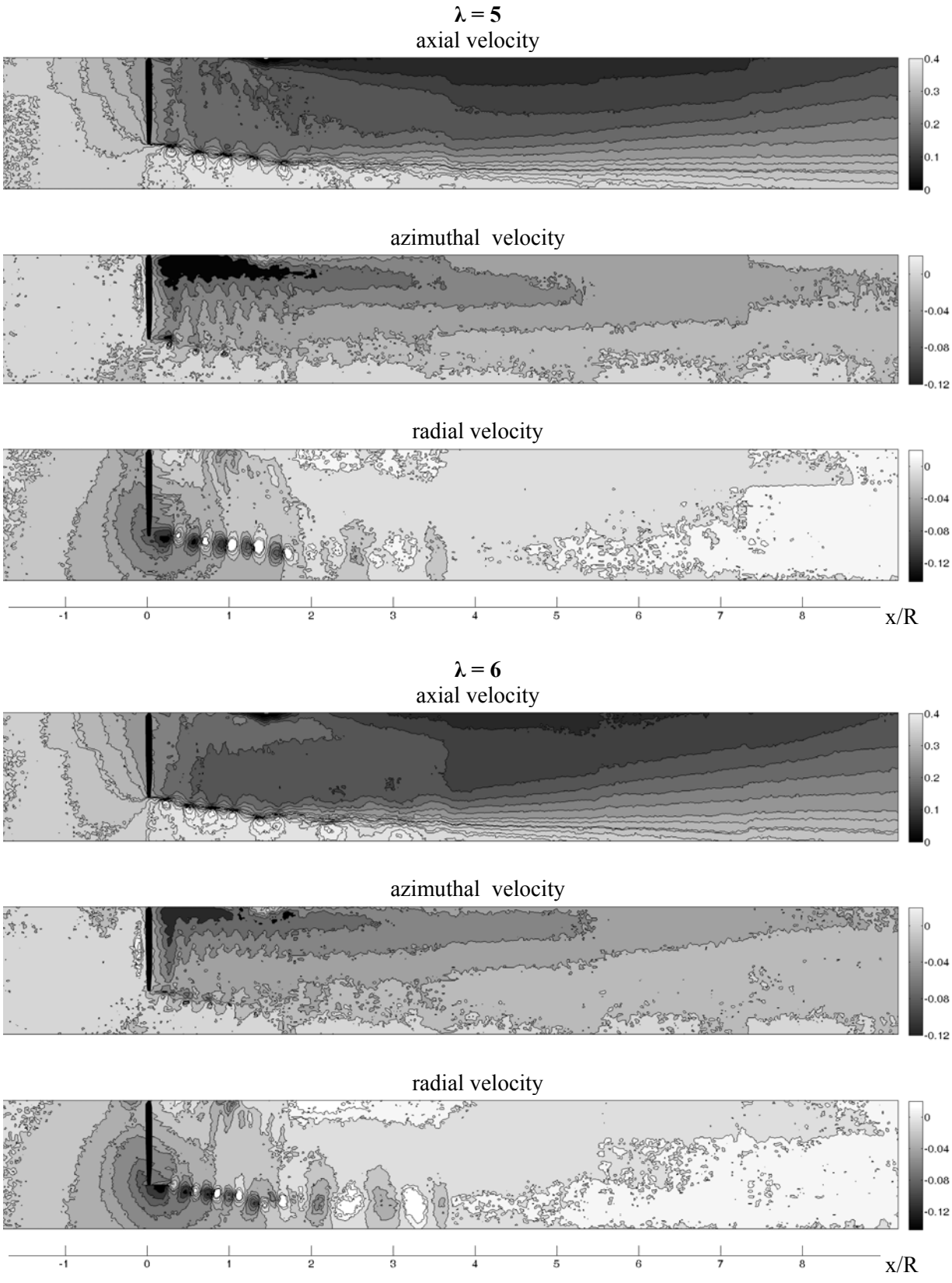

Figure 7. Iso-contours of the phase averaged velocity in the rotor wake

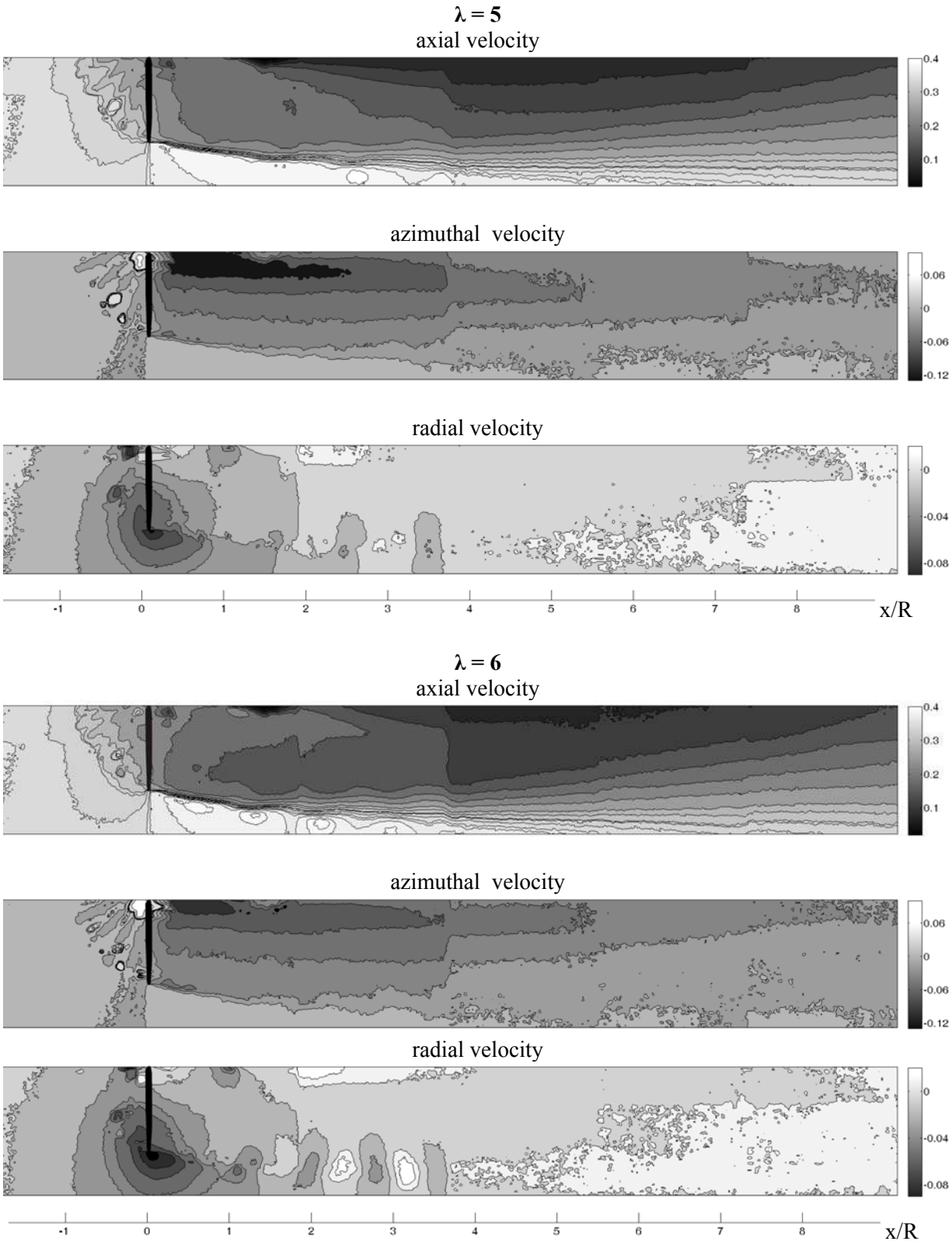

Figure 8. Iso-contours of the ensemble averaged velocity in the rotor wake

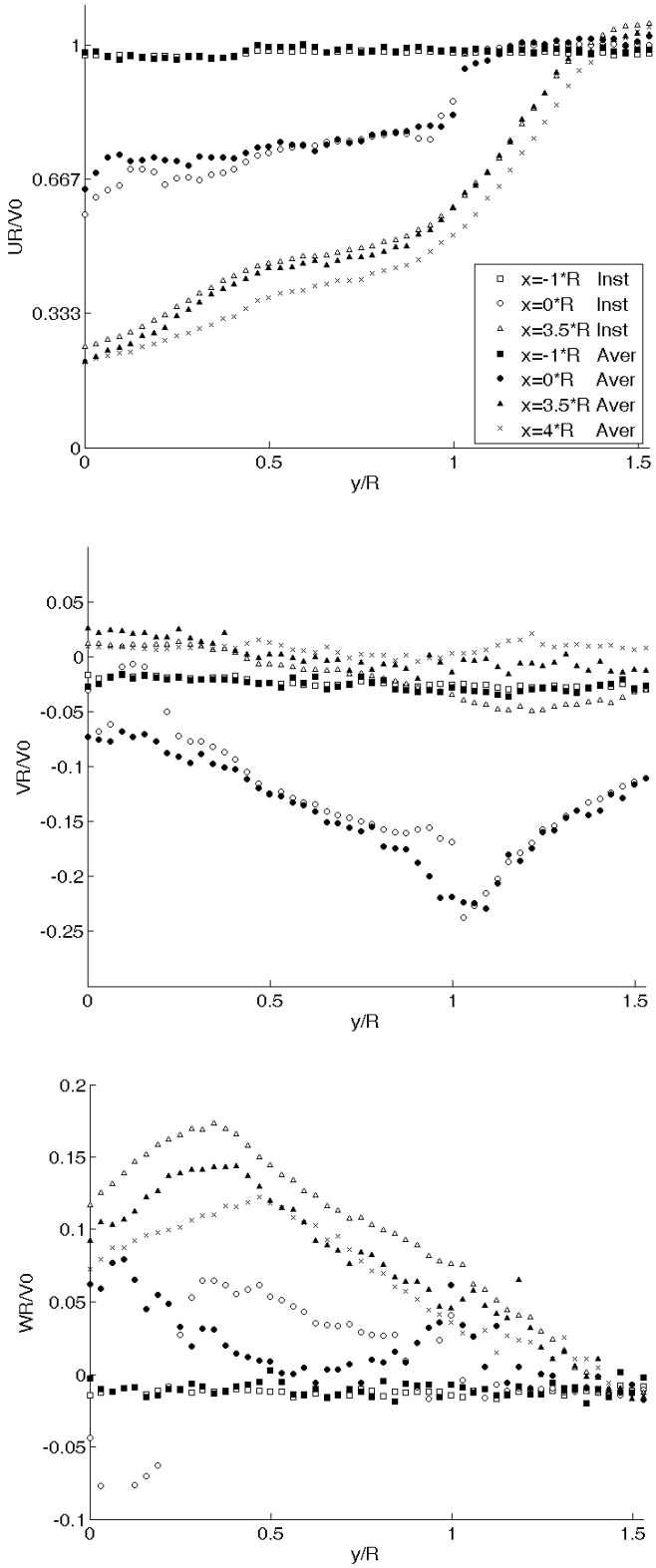

Figure 9. Comparison of the phase averaged and ensemble averaged velocity for $\lambda = 5$, where U- axial, V – radial and W – azimuthal velocity components

Further, Fig. 9 shows a comparison between the phase averaged (Inst) and ensemble averaged (Aver) velocity profiles at same wake cross sections: upstream, downstream and in vicinity of the rotor. In spite of the small difference in the profiles on the Fig. 9 the iso-contour maps for both phase (Fig. 7) and ensemble (Fig. 8) averaged velocity are unlike each other. The results of Fig. 7 expose a complicated vortical structure of the rotor wake which was indicated by visualization above but the pictures of Fig. 8 lost the wake details.

The most predominant structure of the helical tip vortices well pronounce during our visualizations (Fig. 4 and 6) and PIV-samples (Fig. 7) of the axial and radial components of velocity which vortex cores clearly display as a chain of dipole-types regularities. They trace to downstream behind the blade tips and indicate a boundary of the wake. For the azimuthal velocity these features are less pronounced because this component vanishes at the boundary of the wake (Fig. 9). In addition to the tip vortex structure, the PIV-distributions of the azimuthal component show well-pronounced hub vortex around the rotor axis which was absent on the visualizations (Fig. 4 and 6). We observe near the axis a zone with an intense rotation indicated by both phase and ensemble averaged velocity on the PIV-plots, that can be explained by axisymmetric form of the hub vorticity. Another invisible form of the wake is vortex sheet which leaves the blade from the trailing edge along the whole of span. That indicates only by phase averaged PIV-samples (Fig. 7). Here the vortex sheets are observed as periodic upright "tongues" and "bridges" with very nearly the same period in the axial direction downstream the blade. Note that for all tip speed ratio investigated in the study (Tab. 1) we have observed this complex well-pronounced vortex structure which was reproducible and stable only at a downstream distance of about 3-4 radii behind the rotor. Further downstream a transition zone is observed when the tip vortices become unstable, deformed and tend to pairing. The "tongues" and "bridges" of the vortex sheets disappear earlier. This dynamics of rotor wake are observed in visualizations (Fig. 4 and 6) and confirmed by the phase averaged PIV-samples (Fig. 7).

In additional to the analysis of the wake vortex structure we consider a correspondence between the dynamic behavior and the well-known states of the rotor wake. At first we try to define these zones by the deceleration of the axial velocity. For this reason we depicted a change in the average axial velocity for different fixed radii at the axial direction (Fig. 10). Consistent with common knowledge the near wake describes by decrease of the average axial velocity from 2/3 to 1/3 of wind speed ($0 \leq x/R \leq 3.5$); the transition area corresponding to the area where the tip vortices start being destabilized and invariability of the axial velocity ($3.5 \leq x/R \leq 6$), and the turbulent or far wake appears when this velocity increase again.

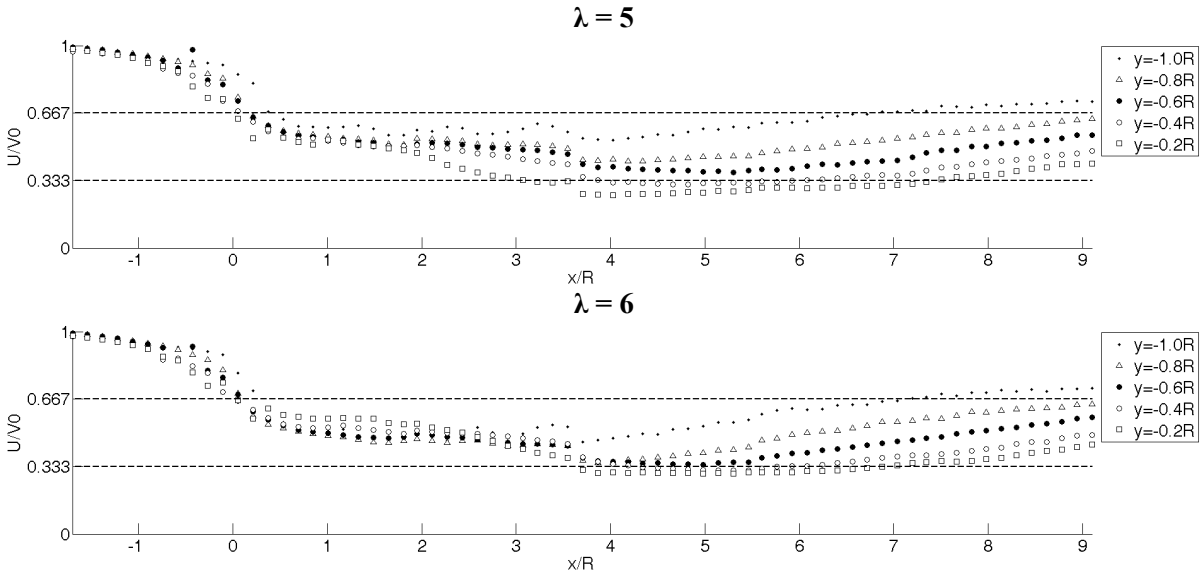

Figure 10. Development of the axial flow deceleration downstream rotor wake for λ = 5 and 6

In keeping with the definition we detected the positions for the first stage from the rotor plane up to 3-4 radii downstream; the second one from the first one up to 6-7 radii and the last one behind 6-7 radii.The comparison with dynamic behavior of the wake reveals that the instability of the vortex structure appears between near and far wakes. In this transition area, the tip vortices are subject to further decay to engender the turbulence wake downstream. It means that far wakes is unstable without domination of well-pronounced stable vortex structures like in the near wake. We can detect this zone only by invariability of the average axial velocity.

Our experimental data permit to test several assumption and conclusions of the well-known rotor theories. This is, for example, confirming Froude's theory [1], which for any optimal rotor predicts the half-deceleration of the axial velocity in the far compared with the rotor plane. Indeed, we have seen that at optimum regime with $\lambda = 5$ the axial velocity in the rotor plane reduces in 1/3 times of wind speed but in the far wake that is 2/3 as it was predicted by Froude's theory and named as Betz limit. Another conclusion of this classical theory is the wake expansion downstream the rotor plane with a factor of 1.22 [21]. Indeed, for the optimal regime $\lambda = 5$ the traces of tip vortices coincided with the wake boundary increases about the same value (Fig. 7).

The main assumption of the rotor theory with a finite number of blades is a proposal about a constant pitch between the tip vortex structures in the axial direction. Both visualization and PIV-sample indicates that the axial distance between cores of two neighboring tip vortices is not subjected to any significant changes and keeps about constant. The same fact was observed downstream a wind turbine model in wind tunnel also [22]. Another important assumption of the analytical model [5] with constant circulation along blade concerns the absence of azimuthal rotation of tip vortices in the wake. Our measurements confirmed that the azimuthal velocity vanishes in the vicinity of the tip vortices. The final interesting conclusion from our measurements concern the confirmation of the instability in far wake, which was before investigated analytically and found unconditionally unstable for the wake structure with tip helical vortices and strong opposite hub vorticity [23]. Indeed, for all operating regimes we observed development of instability of these vortex structures in far wake.

4. Conclusions

The flow behind the model of wind turbine rotor is investigated experimentally in a water flume using Stereoscopic Particle Image Velocimetry. In our instantaneous and averaged 2D-3C PIV-measurements of the velocity field behind model of wind turbine we have found the complex vortex structure of near wake and detected far wake as unstable regime without a regular vortex structure. The transitional regime, generally characterized as in between the regime governed by stable organized vortical structures and the turbulent wake, develops from disturbances of the tip and root vortices through vortex paring and further complex behaviour towards the fully turbulent wake. The near wake characteristics (development of expansion, tip vortex position, deficit velocity and rotation in the wake) have been measured for different tip speed ratio.

Further, using this data we have tested and proved several assumptions and hypothesis of the famous classical rotor theories. The good agreements between our experimental results and the rotor theory with a finite number was found. Our experiment confirms the classical Froude theory and also shows the ability to perform experimental investigation of the wind turbine model in water flume.

5. Acknowledgments

This study was supported in part by the Denmark Energy Agency (project EUDP_2011_J, grant no. 64011_0094) and Ministry of Education and Science of the Russian Federation (project no. 11.519.11.6022). The authors also express their thanks to K.E. Meyer and C.M. Velte for useful discussions and help in calibration of PIV equipments during experiments.

References

[1] Froude R E 1889 On the part played in propulsion by differences of fluid pressure *Trans. Inst. of Naval Architects* **30** 390-405
[2] Joukowsky N E 1913 Vortex Theory of Screw Propellers *Proc. Department of Physics Sciences of the Scientific Society of Natural Science* **16**
[3] Betz A 1919 Schraubenpropeller mit geringstem Energieverlust: mit einem Zusatz von L. Prandtl (Göttingen Nachrichten, Göttingen)
[4] Goldstein S 1929 On the vortex theory of screw propellers *Proc. Roy. Soc. London* **123** 440–465
[5] Okulov V L, Sørensen J N 2010 Maximum efficiency of wind turbine rotors using Joukowsky and Betz approaches *J. Fluid Mech.* **649** 497-508
[6] Okulov V L, Gijs van Kuik A M 2012 The Betz—Joukowsky limit: on the contribution to rotor aerodynamics by the British, German and Russian scientific schools *Wind Energy* **15** 335-344
[7] Flamm O 1909 Die Schiffsschraube und ihre Wirkung auf das Wasser Die Schiffsschraube und ihre Wirkung auf das Wasser - Photo-stereoskopische Aufnahmen unter gleichzeitigen Energie- und Geschwindigkeits-Registrierungen der im Wasser frei arbeitenden Schraube (R. Oldenbourg) 23
[8] Ryabushinsky D P 1908 *Bulletin de l'institute aerodynamique de Koutchino* **2** 32
[9] Vermeer L J, Sørensen J N, Crespo A 2003 Wind turbine wake aerodynamics *Prog. Aerosp. Sci.* **39** 467–510
[10] Alfredsson P H, Dahlberg J A, Vermeulen P E J 1982 A comparison between predicted and measured data from wind turbine wakes *Wind Engineering* **6** 149-155
[11] Ebert P R, Wood D H 1997 The near wake of a model horizontal-axis wind turbine: Part 1: experimental arrangements and initial results *Renew Energ* **12** 225–243
[12] Snel H, Schepers J G, Montgomerie B 2007 The MEXICO (Model Experiments in Control Conditions): the database and first results of the data process and interpretation *J. Physics: Conf. Ser.* **75** 012014
[13] Shen W Z, Zhu W J, Sørensen J N 2012 Actuator line/Navier-Stokes computations for the MEXICO rotor: comparison with detailed measurements *Wind Energy* **15** 811-825
[14] Ciocan G D, Iliescu M S, Vu T C, Nennemann B, Avellan F 2007 Experimental study and numerical simulation of the FLINDT draft tube rotating vortex *J. Fluids Eng.* **129** 146-158
[15] Felli M, Camussi R, Di Felice F 2011 Mechanisms of evolution of the propeller wake in the transition and far fields *J. Fluid Mech.* **682** 5-53
[16] Selig M S, Guglielmo J J, Broeren A P, Giguere P 1995 Summary of low-speed airfoil data *SolarTech Publication* (Virginia Beach: Virginia) **1** p. 292
[17] Glauert H 1935 Airplane propellers *Aerodynamic Theory* ed. W.F.Durand (Berlin: Springer) **IV** 169-360.
[18] Adrian R J 1991 Particle imaging techniques for experimental fluid mechanics *Ann. Rev. Fluid Mech.* **23** 261-304
[19] Okulov V L, Naumov I V, Sørensen J N 2007 Optical diagnostics of intermittent flows *Technical Physics* **77** 47-57
[20] Naumov I V, Okulov V L, Mayer K E, Sørensen J N, Shen W Z 2003 LDA – PIV diagnostics and 3D simulation of oscillating swirl flow in a closed cylindrical container *Thermophysics and Aeromechanics***10** 143-148
[21] Hansen M O L 2008 Aerodynamics of Wind Turbines (London: Earthscan) p 181
[22] Nilsson K, Shen W Z, Sørensen J N, Ivanell S 2011 Determination of the tip vortex trajectory behind the MEXICO rotor *Abstr. Wake Conf. Gotland University* (Visby, Sweden) 94–99
[23] Okulov V L, Sørensen J N 2007 Stability of helical tip vortices in a rotor far wake *J. Fluid Mech.* **576** 1-25